




Research Article

Stability Analysis of the Lining Reinforcement Structure of a Double-Track Heavy-Haul Railway Tunnel

Weibin Ma ^{1,2} Jinfei Chai ^{1,2} Xiaoyan Du ^{1,2} Yao Li,^{1,2}
Peng Zhao,^{1,2} and Shanduo Li^{1,2}

¹Railway Engineering Research Institute, China Academy of Railway Sciences Corporation Limited, Beijing 100081, China

²State Key Laboratory for Track Technology of High-Speed Railway, Beijing 100081, China

Correspondence should be addressed to Jinfei Chai; chaijinfei@rails.cn and Xiaoyan Du; 466074024@qq.com

Received 18 July 2022; Revised 26 October 2022; Accepted 19 April 2023; Published 20 May 2023

Academic Editor: Jianyong Han

Copyright © 2023 Weibin Ma et al. This is an open access article distributed under the Creative Commons Attribution License, which permits unrestricted use, distribution, and reproduction in any medium, provided the original work is properly cited.

An increasing number of railway tunnels are afflicted with railway tunnel lining diseases. Through on-site detection of lining diseases in double-track railway tunnels, this paper analyzed its causative factors and developed a section steel arch frame lining reinforcement. Through a simulation of its mechanical performance, both the steel plate and concrete met the tensile strength code requirements for railway tunnel design (TB 10003-2016). It effectively repaired the damage from lining diseases under narrow-site and short maintenance “window” time conditions without affecting the normal operation of catenary and power supply facilities. This reinforcement has great practical significance and broad application prospects.

1. Introduction

By the end of 2021, China’s railway network reached 145,000 km, which includes 17,532 railway tunnels having a combined length of about 21,055 km [1]. As the train axle load and transportation density increase, so do the dynamic-load strength and fatigue effect of heavy-duty railway tunnels. In addition, seismic disturbances and corrosion from water and salt increase the probability of structure diseases; in fact, many tunnel linings have cracks, blocks, and voids. In addition, the dynamic stress and vibrations of the heavy-vehicle and light-vehicle lines unbalance the double-track heavy-haul railways, resulting in a deteriorating lining, which affects the train’s long-term operational safety [2].

Ma et al. tested the in situ stress distribution of the railway tunnels in Southwest China based on the complete temperature compensation technology. Ma et al. [3] analyzed the vibration law of railway tunnel substructure under different axle loads and health conditions, and Ma et al. [4] researched the design parameters and fatigue life of tunnel bottom structure of single-track ballasted heavy-haul railway tunnel with 40-ton axle load [5]. Han et al. [6] developed a treatment technology for

optimizing the stress state of railway tunnel bottom structure. Chai [7, 8] analyzed the dynamic response characteristics for basement structure of heavy-haul railway tunnel with defects and researched the multijoint rock failure mechanism based on moment tensor theory.

Zhao [9] divided the crack reinforcement of a railway tunnel lining into crack treatment and structural reinforcement. Cracks with a small width and no penetration are generally filled with epoxy resin or mortar. Grout, shotcrete, or reinforced concrete behind the lining is used on wide, penetrating cracks. For a lining structure without a load-bearing capacity, it is removed and a new lining is reconstructed. Cheng et al. [10] divided tunnel cracks into four grades according to width and length: AA, A1, B, and C, from heavy to light. They proposed that grade AA be reinforced by W-shaped steel-belted mesh shotcrete; grade A1 by cross-seam anchor-bolt grouting; and the lighter-grade B and C cracks by appropriate shotcrete. Because the code has strict provisions regarding the effective clearance area of a high-speed railway tunnel, reinforcement measures should not be adopted when repairing cracks. Therefore, Cheng [11] put forward treatment measures for different levels of cracks.

In view of the deficiency in lining thickness and strength, Niu et al. [12] proposed structural reinforcement in the form of anchor spraying or sticking fiber cloth with a steel plate inside. In addition, Yu [13] summarized and pointed out that backfill grouting measures are generally adopted for small cavities behind the railway tunnel lining, while arch sleeve reinforcement is generally adopted for large cavities. Ma et al. [14] proposed that a corrugated steel plate has certain advantages, such as good ductility, for strengthening railway tunnels and can be applied to sections that have large deformations. In general, for some minor diseases such as cracks and cavities, grouting backfill reinforcement is generally carried out. For diseases of great structural impact, secondary reinforcement by means of an arch covering or pasted steel plates for backfilling is required. Wu et al. [15] and Cheng et al. [16] developed the hybrid complex variable element-free Galerkin method for 3D elasticity problems. Li and Wu [17] studied the basic formula of elastoplastic damage constitutive model of concrete.

Finding an effective means of repairing the lining of narrow, double-track heavy-haul railway tunnels that have limited maintenance “window” time, without affecting the normal operation of catenary and power supply facilities, is an urgent problem. Therefore, conducting research into current lining methods is of great practical significance and could have broad application.

To address these lining diseases, this paper is divided as follows. Section 1 introduces previous research results. Section 2 introduces the general situation of tunnel and lining diseases. Section 3 offers a preliminary analysis of the causes of tunnel lining diseases through data collection, field investigation, and detection. Section 4 introduces the design principles and maintenance methods of a reinforced steel arch frame lining. Section 5 analyzes the steel arch frame reinforcement using a numerical simulation. Section 6 draws conclusion and offers suggestions for further research.

2. Project Overview

Daheishan Tunnel, completed in 1984 under the management of the Chawu Railway Engineering Section of a heavy haul railway in northern China, is located between Yanqing North Station and Xiazhuang Station northeast of the Changping District of the Daqin Railway. It is a double-track tunnel.

The center mileage is K 299 + 700, with a total length of 2715 m. The lining of the tunnel is mainly a curved wall structure, and the line is downhill 10.1–10.8‰ in the direction of tunnel exit. The tunnel passes through the main peak of Daheishan mountain in the Yanshan Mountains, and all the tunnels pass through the Yanshanian granite layer. It is a gray-yellow, flesh-red medium grain structure on complex terrain and developed gullies. The maximum buried depth of the tunnel is 303 m. The lining was constructed according to the special tunnel 0025 drawing. It is a double-track electrified tunnel with curved wall concrete masonry.

The transportation load of this line is heavy, and the Daheishan Tunnel has been in operation for nearly 40 years. Over that time, its structural concrete has deteriorated

severely. In March 2021, according to data provided by the tunnel management and maintenance unit and through geological radar detection and three-dimensional laser scanning, it was found that the lining of the tunnel 1605–1625 m away from the tunnel entrance had cavities, falling blocks, wrong platforms, and other diseases seriously affecting driving safety, as shown in Figure 1. The size of the cavity opening is $0.1 \times 0.8 \times 0.3$ m; the thickness of lining concrete is about 30 cm; the deterioration is serious; and no reinforcement was found. The depth of the cavity was about 1 m and extended for 10 m in the direction of tunnel entrance. According to the *Evaluation Standard for Deterioration of Railway Bridge and Tunnel Buildings Part 2: Tunnel* (Q/CR 405.2-2019) of China, the disease grade was evaluated as AA, which meant treatment had to be taken immediately because of the risk to traffic safety (see Figures 2 and 3).

3. Cause Analysis of Lining Disease

By means of data collection, field investigation, and detection, the preliminary analysis showed that the causes of lining disease are as follows:

- (1) *Design Factors.* Tunnel construction began in the 1980s, and there was a large gap between the design standard and the engineering technology of the time, which was generally low.
- (2) *Construction Factors.* To reduce the amount of shotcrete after tunnel overbreak, during shotcrete construction, surrounding loose rock was not cleared in place, resulting in a cavity not being fully back-filled behind the initial support; as a result, the performance of the concrete lining was poor. The construction quality was also poor and insufficiently thick. With the progress of geological changes, the rock blocks above the cavity suddenly failed to support the concentrated load, causing the lining to break, resulting in falling blocks, a cavity, and other problems.
- (3) *Deterioration Factors.* The tunnel is nearly 40 years old, and as its lining concrete continues to deteriorate, its bearing, bending, and shear capacity declines. Under continuous rock pressure, the deteriorating thin lining shell cracks, leading to falling blocks and cavities.
- (4) *Fault Factor.* The diseased lining section crosses the reverse fault, and fault activity leads to stress changes around the tunnel.
- (5) *Influencing Factors of Train Load.* The vibration of heavy-haul trains is considerable and causes the lining concrete to crack easily.

4. Design Principles and Maintenance Method

4.1. Design Principles. Due to limited operating space, poor working environment, and safety of the operating line tunnel, disease treatment is a very complex project.



FIGURE 1: Real map of lining diseases of Daheishan Tunnel on Datong to Qinhuangdao Railway.

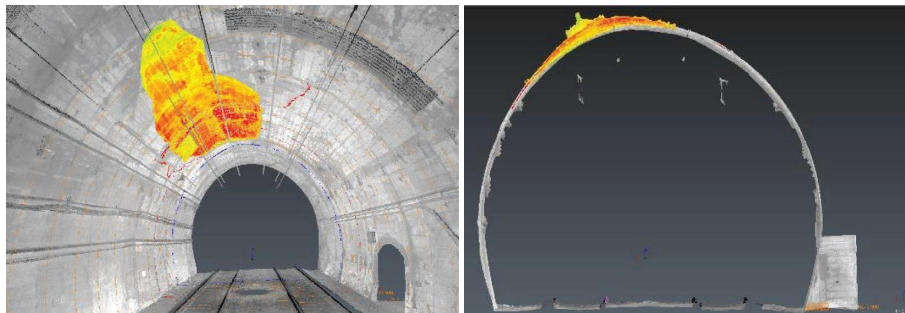


FIGURE 2: Three-dimensional laser scan of lining diseases in Daheishan Tunnel on Datong to Qinhuangdao Railway.

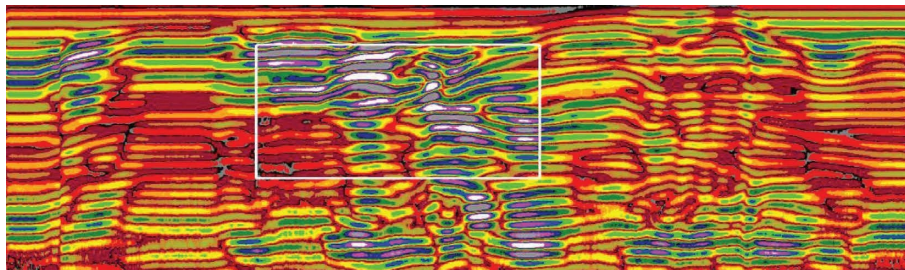


FIGURE 3: Geological radar detection of lining disease of Daheishan Tunnel on Datong to Qinhuangdao Railway.

Therefore, the following principles concerning tunnel reinforcement construction organization design had to be followed:

- (1) Given the current state of tunnel diseases, the reinforcement design was carried out to ensure safe operation of the line.
- (2) Factors such as the construction environment and amount of daylight were considered to minimize the influence on normal operation of the line as far as possible.
- (3) The state of the surrounding rock and tunnel structure had to be under constant observation, and increased monitoring and measurement were done if necessary.
- (4) Because of the complexity, particularity, and uncertainty of tunnel engineering construction, close communication and cooperation among the construction, design, equipment management, and other units were required, and construction was adjusted as necessary to match the actual conditions.
- (5) The construction scheme was controlled according to the comprehensive minimum construction clearance size of Daheishan Tunnel.
- (6) The insulation distance between temporary and permanent measures and the electrified body had to meet the requirements set out in the Code for Design of Railway Electric Traction Power Supply (TB10009-2016).
- (7) During construction, the cables in the diseased section had to be effectively protected.

4.2. Remediation Plan

4.2.1. Technical Introduction. To prevent further cracking and deformation of the tunnel lining or serious water leakage, arch reinforcement was performed: an arch

structure was added along the surface of the original lining to form a common bearing body with the original lining. It is the most effective method for solving serious lining leakage because it gives good reinforcement, and construction quality is easy to control.

The main content of the treatment plan is to add circumferential H-shaped steel on the lining surface, weld steel plates between the H-shaped steel on the side away from the lining, and fill concrete between the steel plate and the lining.

The specific measures were as follows. An H175 steel arch frame was erected on the inner side of the lining according to the clearance requirements, and spacing of the steel arch frame was 1.0 m. The two steel arches were longitudinally connected with 20 mm in diameter deformed steel bars. The circumferential spacing was 1 m. Deformed steel bars were connected longitudinally with a circumferential spacing of 1 m; short anchor bolts were constructed between the steel arches; circumferential reinforcing mesh was erected; cavity grouting behind the lining was carried out; 6 mm thick steel plates were welded, and C35 concrete was poured inside, as shown in Figures 4 and 5.

4.2.2. Specific Steps

- (1) During construction, the loose concrete lining was chiseled out; the concave groove was excavated at the erection position on the top surface of the tunnel trench; and the footing was used to support the grouting anchor pipe. The erection steel plate was welded at the end of the anchor pipe. After erecting the H175 steel arch, drill and install the anchor bolt and weld the end of the anchor bolt to the steel arch. Then, the micro-expansion concrete was filled manually behind the flange of the H-steel arch to ensure that the steel arch was close to the original lining.
- (2) The H-shaped steel arch frame was processed outside the tunnel in five sections and assembled in the tunnel. The steel at both ends was connected with a 1 cm thick steel plate and high-strength bolts at the section connection and was firmly welded. The section length of the H-shaped steel arch frame was appropriately adjusted according to different mileage and sections.
- (3) Before grade II welding, rust spots at the welding position had to be cleared, and there had to be no pores, undercuts, cracks, or other phenomena during welding. All welds were fully welded.
- (4) In addition to chiseling the loose and cracked concrete in the reinforced section of the steel arch frame, it also had to be chiseled in combination with the tunnel clearance to embed the frame.
- (5) Drill holes at the foot of the wall using a down-the-hole drill, lock the steel arch frame in the depth of the surrounding rock using anchor pipes and anchor rods, transfer as much load as possible to the deep part of the surrounding rock, and clean the connection between the steel arch frame, steel plate, and anchor pipe.
- (6) After the steel arch frame was erected, M20 cement mortar was used to fill the chisel groove and the gap between the profile steel flange and the concrete lining surface to bring the frame close to the original concrete lining and give full play to its bearing capacity.
- (7) Inspect the welds between the sections of the original steel arch and repair and strengthen those that failed to meet the requirements.
- (8) Short anchor bolt with 20 mm in diameter threaded reinforcement with a circumferential spacing of 0.5 m was welded with steel plate and anchored in the lining using a coil anchoring agent.
- (9) Erect three steel arches between two adjacent steel arches (20 mm in diameter) to form a circumferential reinforcement mesh.
- (10) Grout the cavity behind the lining by a small conduit (42 mm in diameter) that injected micro-expansion material with a grouting pressure of 0.3 MPa.
- (11) Remove the loose concrete between the arch frame and the lining, roughen and clean the tunnel lining surface, and then brush with a concrete interface agent.
- (12) Erect the steel plate from bottom to top from the top surface of the tunnel trench. Weld the steel plate on the inner side of the outer edge of the section steel and at the end of the short anchor bolt. Weld the plate with a ring spacing of 0.5 m in diameter. Weld the steel plate with a flange of the steel arch frame with a length of 100 cm and a circumferential width of 500 cm. Bend the steel plate according to the radian of the steel arch frame on site. After each steel plate was installed, vibrate C35 concrete filled in the space between the steel plate and the original lining to ensure filling.
- (13) Remove rust, polish, and spray red lead primer on exposed steel members and then brush dark gray antirust paint twice.

4.3. Mechanical Analysis Method of Steel Arch Structure.

Taking the stress condition of the circular arch as an example, the internal force was calculated and solved (see Figures 6 and 7). As shown in Figure 8, the arch was divided into n segments, where C_i represents the i th segment from bottom to top; the stiffness is E_i ; the node length is expressed as L_i ; and the arch crown had no nodes. The semistructural analysis is shown in Figure 9.

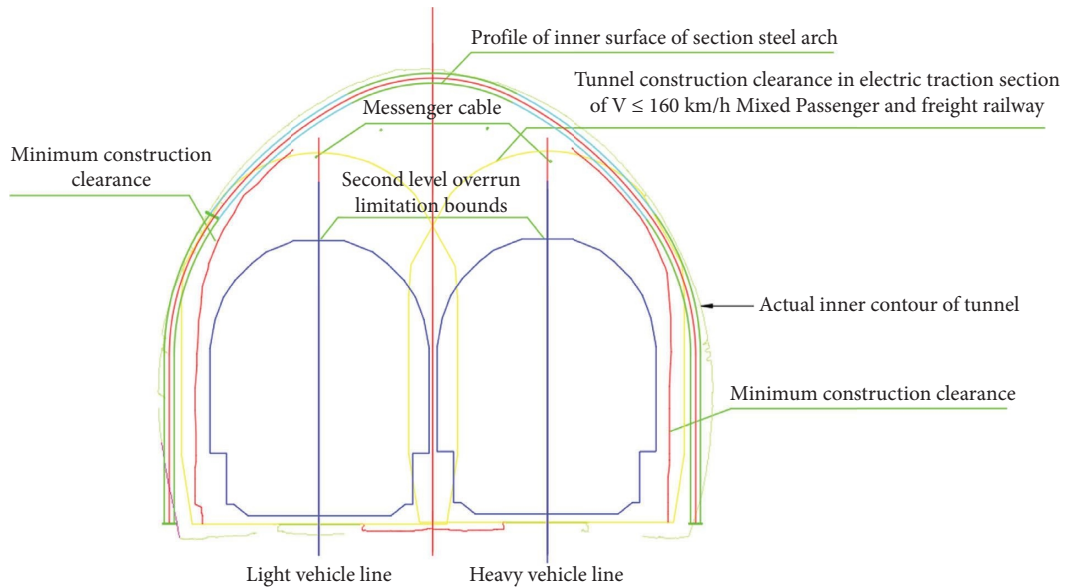


FIGURE 4: Gauge comparison.

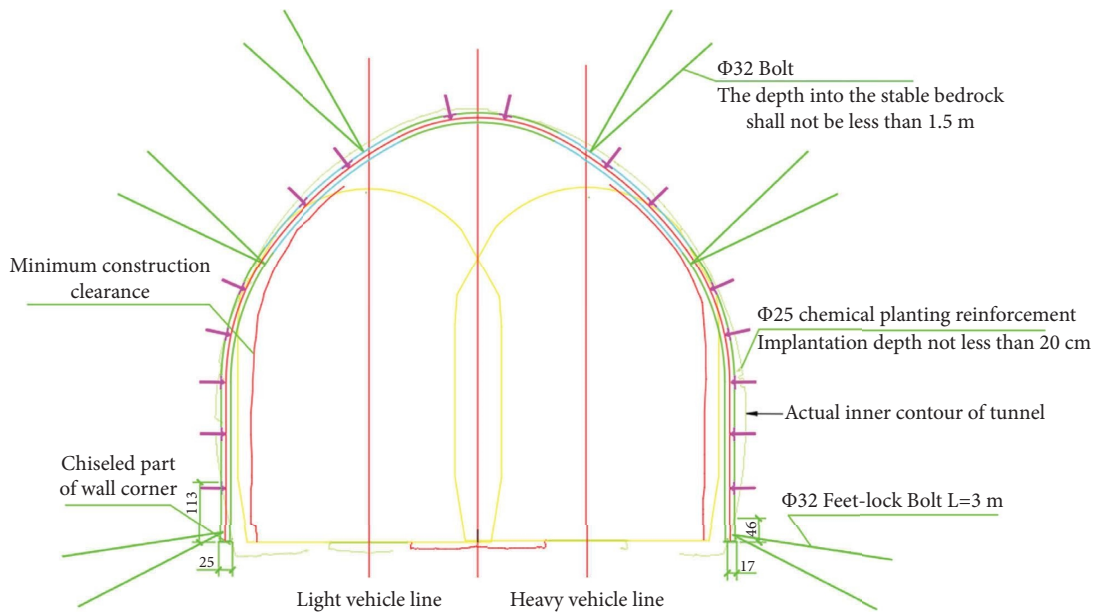


FIGURE 5: Overall cross section layout.

4.4. Establishing Equilibrium Equation. The half structure of the steel arch structure is a statically indeterminate structure, and the internal force of the statically indeterminate structure was solved according to the force method. The equation established by the external force balance condition of the structure is as follows:

$$\begin{cases} F_{Ax} = F_{Cx} = q_2 R, \\ M_A = M_C. \end{cases} \quad (1)$$

4.4.1. Establishing Force Method Equation. Take M_c as the redundant unknown force and M_1 as the basic unknown

force, and the force method equation is shown in the following formula:

$$\delta_{11} M_1 + \Delta_{1P} = 0. \quad (2)$$

4.4.2. Solving Δ_{1P} . According to the generalized diagram multiplication method, only internal forces caused by bending moments are considered, so the following is obtained:

$$\nabla_{1P} = \int \frac{M\bar{M}}{EI} ds. \quad (3)$$

According to the calculus formula, the accumulated displacement of each segment is added to obtain

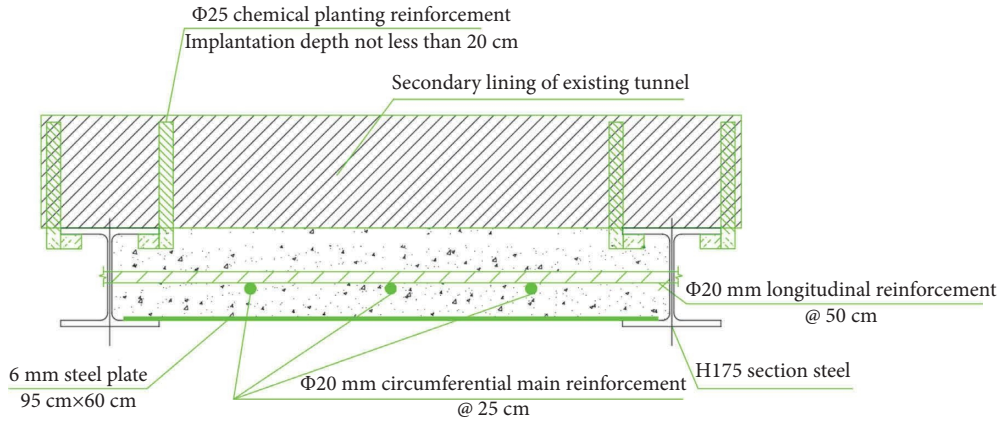


FIGURE 6: Structural cross section design drawing.

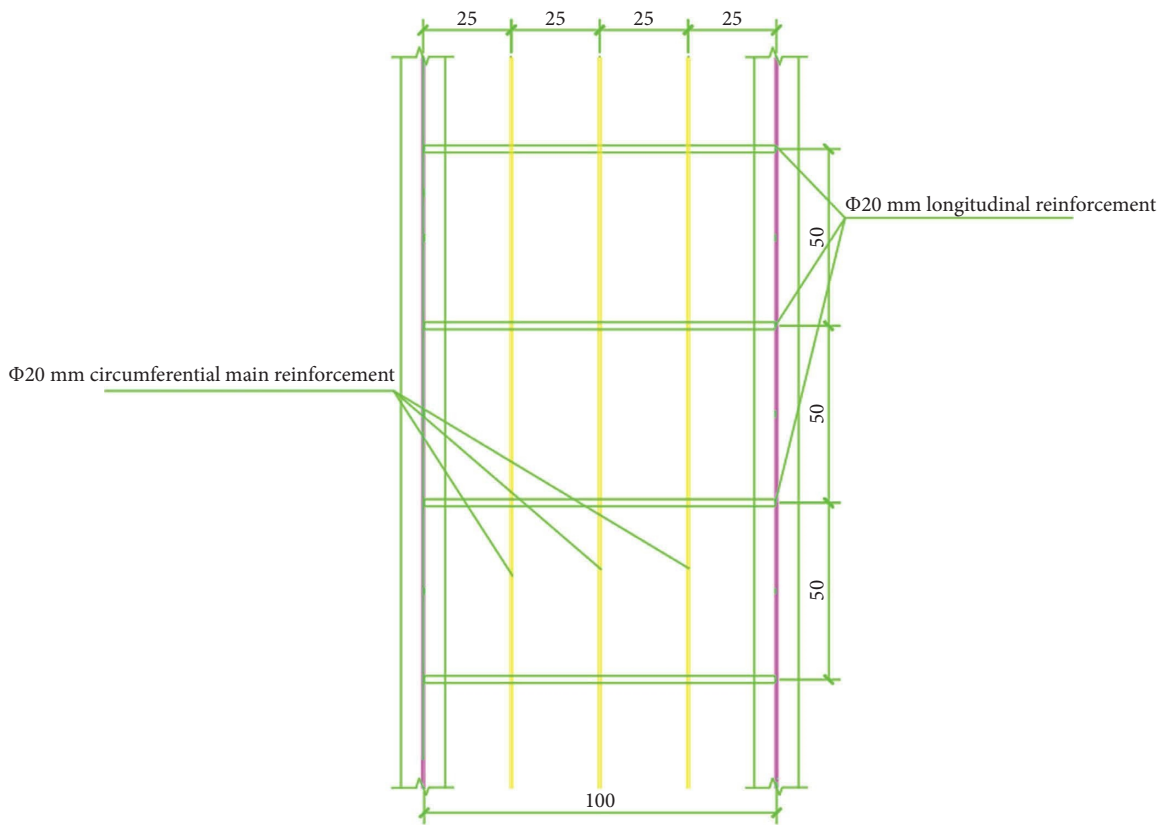


FIGURE 7: Reinforcement layout drawing.

$$\Delta_{1P} = \int \frac{M\bar{M}}{EI} ds = \int_0^{\theta_1/2} \frac{M\bar{M}}{EI_1'} Rd\varphi + \int_{\theta_1/2}^{\alpha_2 - \theta_1/2} \frac{M\bar{M}}{EI} Rd\varphi + \dots + \int_{\alpha_2 - \theta_1/2}^{\alpha_2 + \theta_1/2} \frac{M\bar{M}}{EI_1'} Rd\varphi + \int_{\alpha_i + \theta_i/2}^{\alpha_{i+1} - \theta_{i+1}/2} \frac{M\bar{M}}{EI} Rd\varphi + \dots + \int_{\alpha_n + \theta/2}^{\pi} \frac{M\bar{M}}{EI} Rd\varphi, \tag{4}$$

of which the radius of steel arch section $L_i = R_i \cdot \theta_i$ is

$$\theta_1 = \theta_2 = \dots = \theta_n = \theta. \tag{5}$$

The equivalent bending stiffness of the segment is

$$EI_1' = EI_2' = \dots = EI_i' = \dots = EI_n'. \tag{6}$$

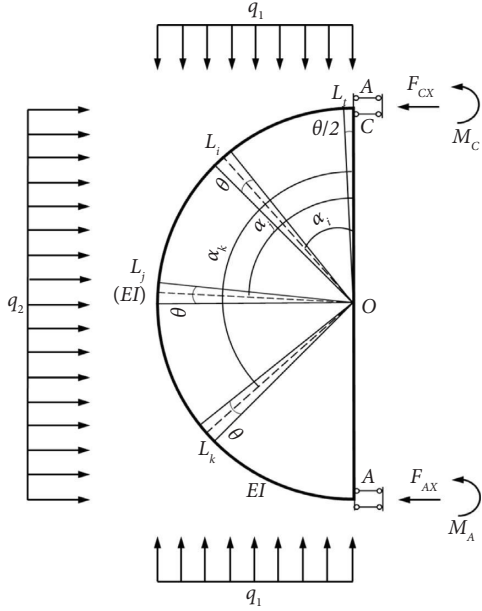


FIGURE 8: Stress analysis diagram.

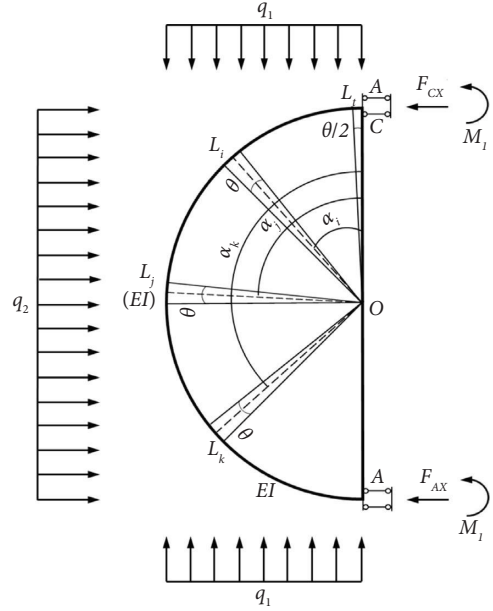


FIGURE 9: Basic system of force method.

So, equation (3) can be simplified as

$$\Delta_{1P} = \sum_1^m \int_{\alpha_i - \theta/2}^{\alpha_i + \theta/2} \frac{M\bar{M}}{EI'_i} R d\varphi + \int_{\alpha_i + \theta/2}^{\alpha_{i+1} - \theta/2} \frac{M\bar{M}}{EI} R d\varphi, \quad (7)$$

of which $\alpha_1 = \theta_1/2$, $\alpha_{n+1} - \theta_{n+1} = \pi/2$.

4.4.3. Solving δ_{11}

$$\delta_{11} = \int \frac{M\bar{M}}{EI} ds. \quad (8)$$

Accumulating the integral by segment number gives

$$\delta_{11} = \int \frac{M\bar{M}}{EI} ds = \sum_1^m \int_{\alpha_i - \theta/2}^{\alpha_i + \theta/2} \frac{M\bar{M}}{EI'_i} R d\varphi + \int_{\alpha_i + \theta/2}^{\alpha_{i+1} - \theta_{i-1}/2} \frac{M\bar{M}}{EI} R d\varphi, \quad (9)$$

in which $\alpha_1 = \theta_1/2$, $\alpha_{n+1} - \theta_{n+1} = \pi/2$.

In general, for the convenience of design and construction, a unified arc length segment was adopted so that $\theta_1 = \theta_2 = \dots = \theta_n = \theta$.

The equivalent bending stiffness of the segment is $EI'_1 = EI'_2 = \dots = EI'_i = \dots = EI'_n$.

4.4.4. Solving Support Reaction. Substitute equation (9) into equation (3) to obtain the unknown force M_C and bring it into the balance equation (10) to obtain the reaction force M_C of other supports.

$$[K]\{\delta\} = \{P\}, \quad (10)$$

where $[K]$ is the overall stiffness matrix of lining structure; $\{\delta\}$ is the node displacement matrix of lining structure, $\{\delta\} = [\delta_1 \delta_2 \delta_m]^T$; and $\{P\}$ is the lining node load matrix $\{P\} = [P_1 P_2 P_m]^T$. In the structural calculation, the structure was generally divided into many micro-elements, and the local element stiffness $[K]^e$, element displacement $\{\delta\}^e$, and element load matrixes $\{P\}^e$ were established. Finally, the element stiffness, displacement, and load matrixes were assembled into the overall stiffness, displacement, and overall load matrixes, respectively.

4.4.5. Internal Force Solution. After the bearing reaction was obtained, the axial force and bending moment of the internal force of each element was solved as

$$F_{N\varphi} = F_{CX} \cos \varphi + q_1 R \sin^2 \varphi - q_2 R \cos \varphi (1 - \cos \varphi), \quad (11)$$

$$M_\varphi = M_C + F_{CX} R (1 - \cos \varphi) - \frac{1}{2} q_1 R^2 \sin^2 \varphi - \frac{1}{2} q_2 R^2 (1 - \cos \varphi)^2.$$

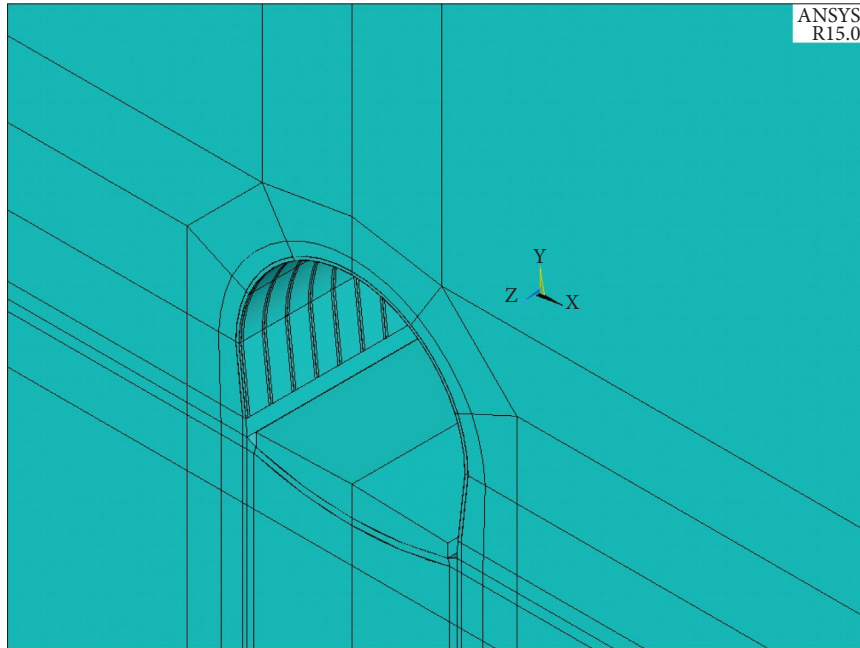


FIGURE 10: Numerical model.

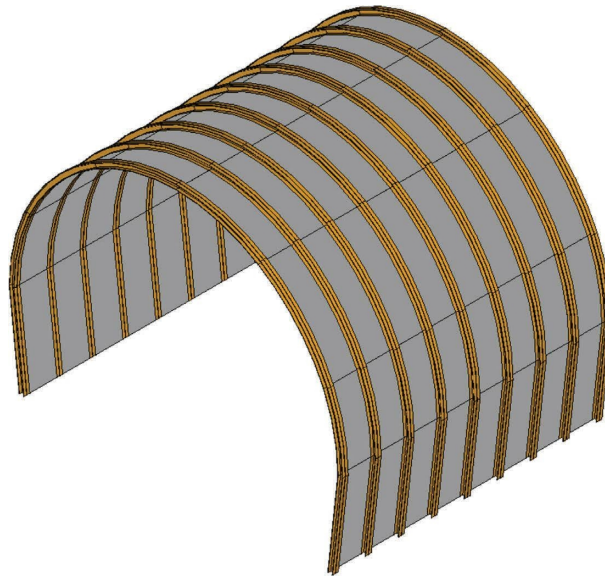


FIGURE 11: Steel frame and steel plate assembly.

4.5. Boundary Conditions. The left and right sides, bottom, front, and rear are fixed constraints.

4.6. Model Dimensions. The dimensions were 16 m along the longitudinal direction of the tunnel, 4 times the tunnel diameter on both sides, 2 times the tunnel diameter at the bottom, and the value at the top taken according to the actual buried depth. The model is shown in Figures 8–11.

4.6.1. Material Parameters. The surrounding rock parameters were selected according to the intermediate value of class IV in the *Code for Design of Railway Tunnel of China* (TB 10003-2016) (see Tables 1 and 2).

The existing structural C30 concrete was selected after being weakened by 50%. The parameters of a newly poured C30 concrete structure were selected according to the equivalent elastic modulus of internal reinforcement.

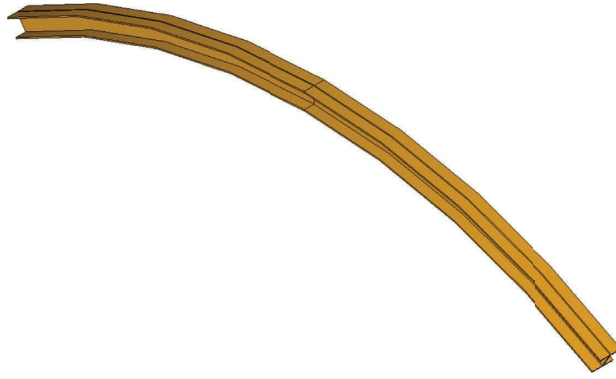


FIGURE 12: Steel frame model.

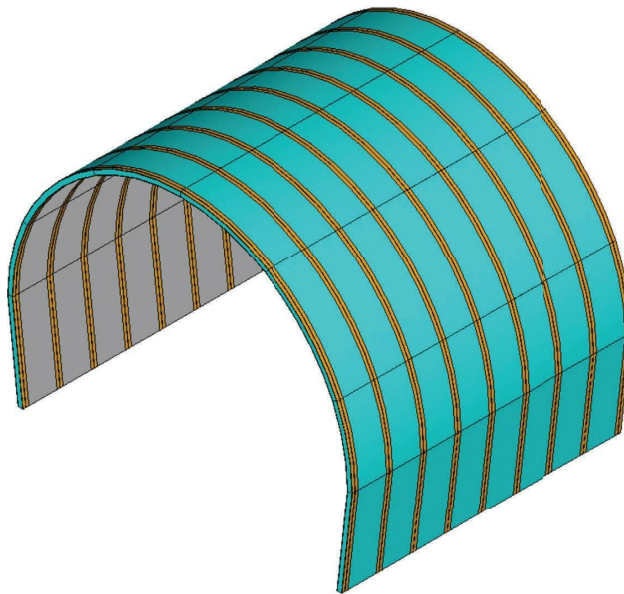


FIGURE 13: Steel frame steel plate concrete composite model.

The steel frame parameters were selected according to the code for railway tunnel design (TB 10003-2016).

4.6.2. Analysis Results

① H175 Steel Frame (Spacing: 1.0 m)

The maximum tensile stress of the steel frame was 28.9 MPa, which occurred at the top of the side wall, meeting the specification requirements (Figure 12).

The maximum tensile stress of the steel plate was 3.09 MPa, which occurred at the bottom of the side wall, meeting the specification requirements (Figure 13).

The maximum tensile stress of the newly poured concrete structure was 2.03 MPa, which occurred at the top of the side wall. It met specification requirements but was close to the tensile limit of the concrete.

② H125 Steel Frame (Spacing: 1.0 m)

The maximum tensile stress of the steel frame was 30.9 MPa, which occurred at the top of the side wall, meeting the specification requirements (Figure 14).

The maximum tensile stress of the steel plate was 3.42 MPa, which appeared at the bottom of the side wall, meeting the specification requirements (Figure 15).

4.7. Application Effect. In 2021, after the Daheishan Tunnel was reinforced with the lining steel arch frame structure (Figures 16 and 17), the crack and cavity of the tunnel lining were effectively repaired; the service capacity of the lining structure was effectively improved; the speed limit of the train in the diseased section was lifted; and the train returned to normal operation (see Figures 18 and 19).

TABLE 1: Parameters of surrounding rock.

Surrounding rock level	Bulk density γ (kN/m ³)	Elastic reaction coefficient K (MPa/m)	Deformation modulus E (GPa)	Poisson ratio ν	Internal friction angle φ (°)	Cohesion c (MPa)	Calculated friction angle φ_c (°)
IV	20–23	200–500	1.3–6	0.3–0.35	27–39	0.2–0.7	50–60

TABLE 2: Material parameters.

Project	Elastic modulus (GPa)	Poisson ratio	Ultimate tensile value (MPa)	Density (kg/m ³)
Existing concrete lining	15.75	0.2	1.1	2500
Fresh concrete	31.5	0.2	2.2	2500
Steel frame	210	0.3	420	7850

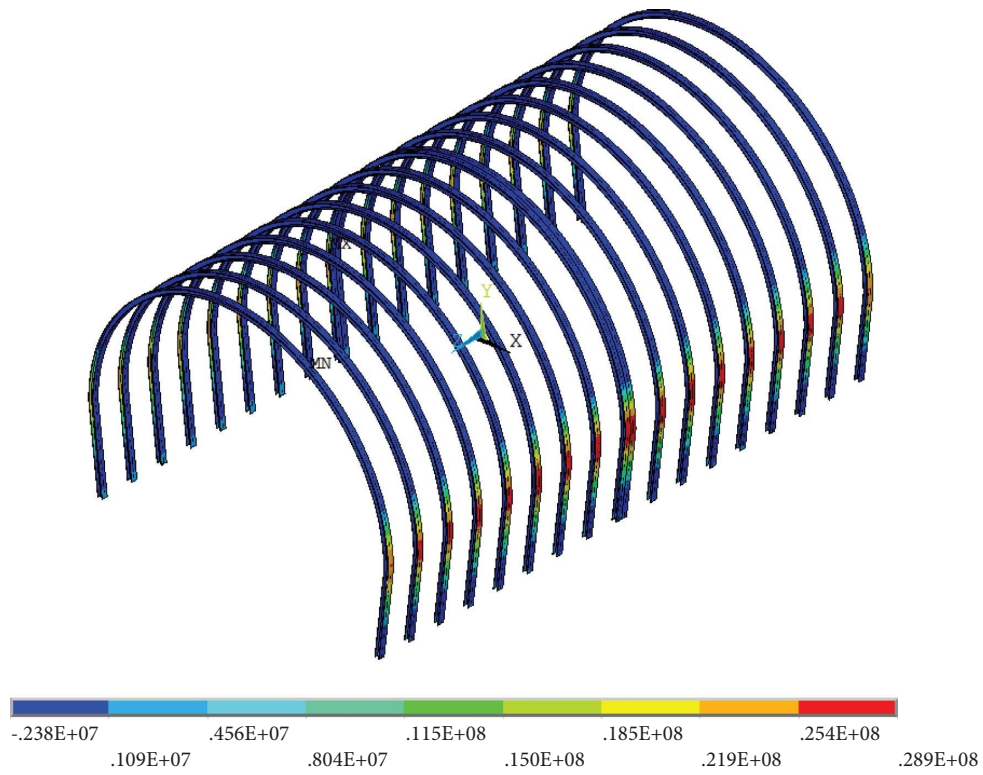


FIGURE 14: Stress diagram of steel frame with H175 steel.

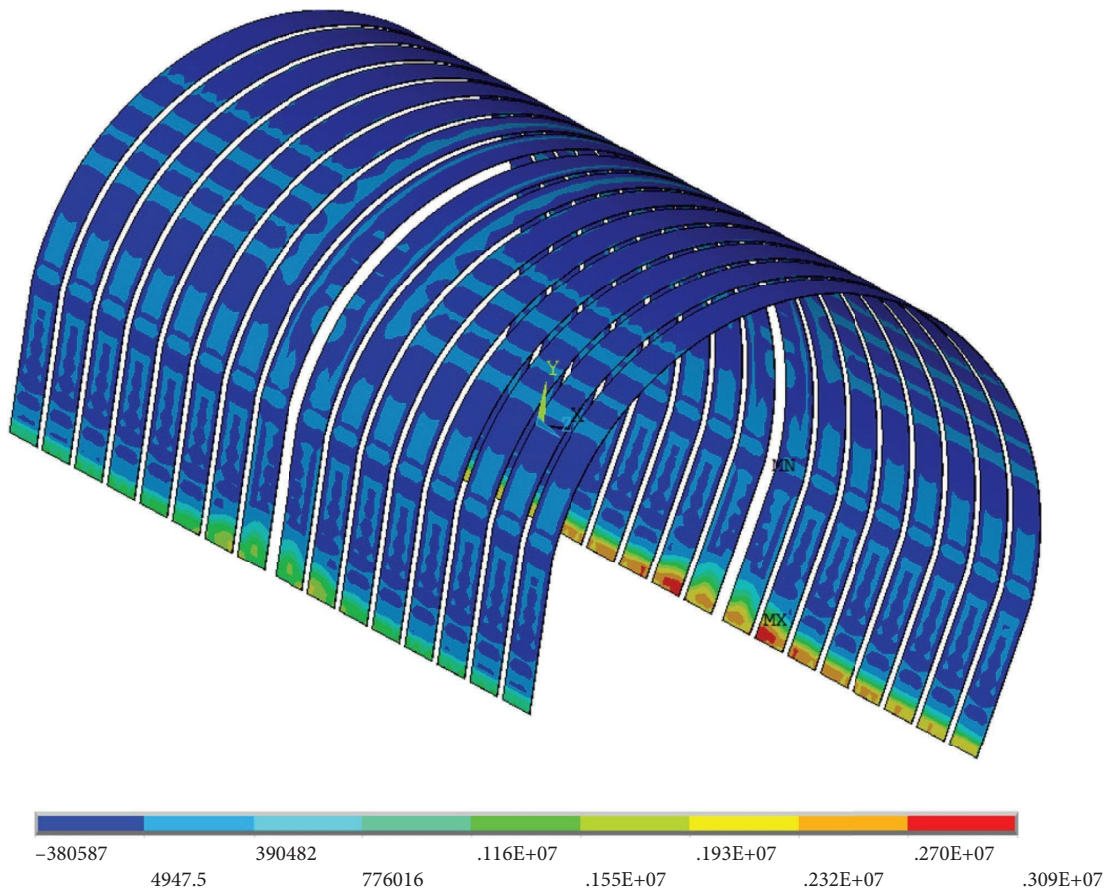


FIGURE 15: Stress diagram of steel plate with H175 steel frame.

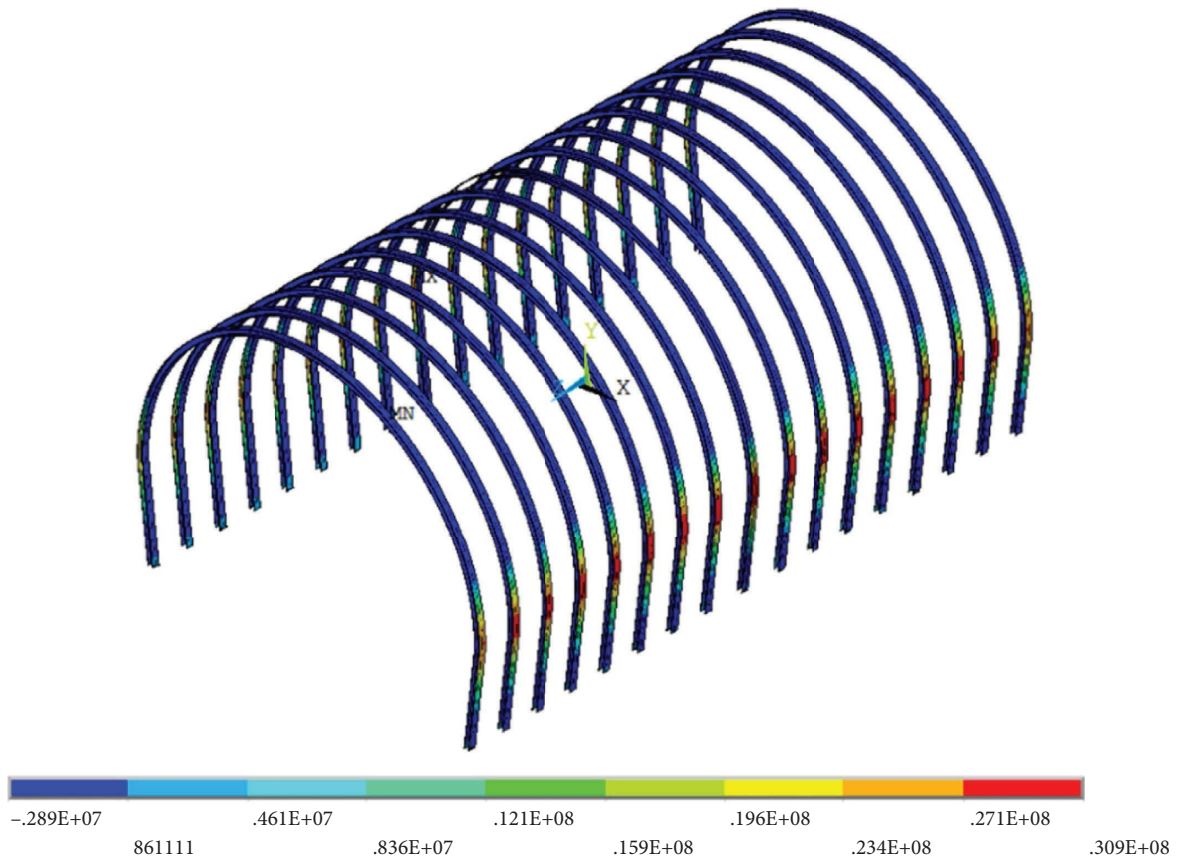


FIGURE 16: Stress diagram of steel frame with H125 steel frame.

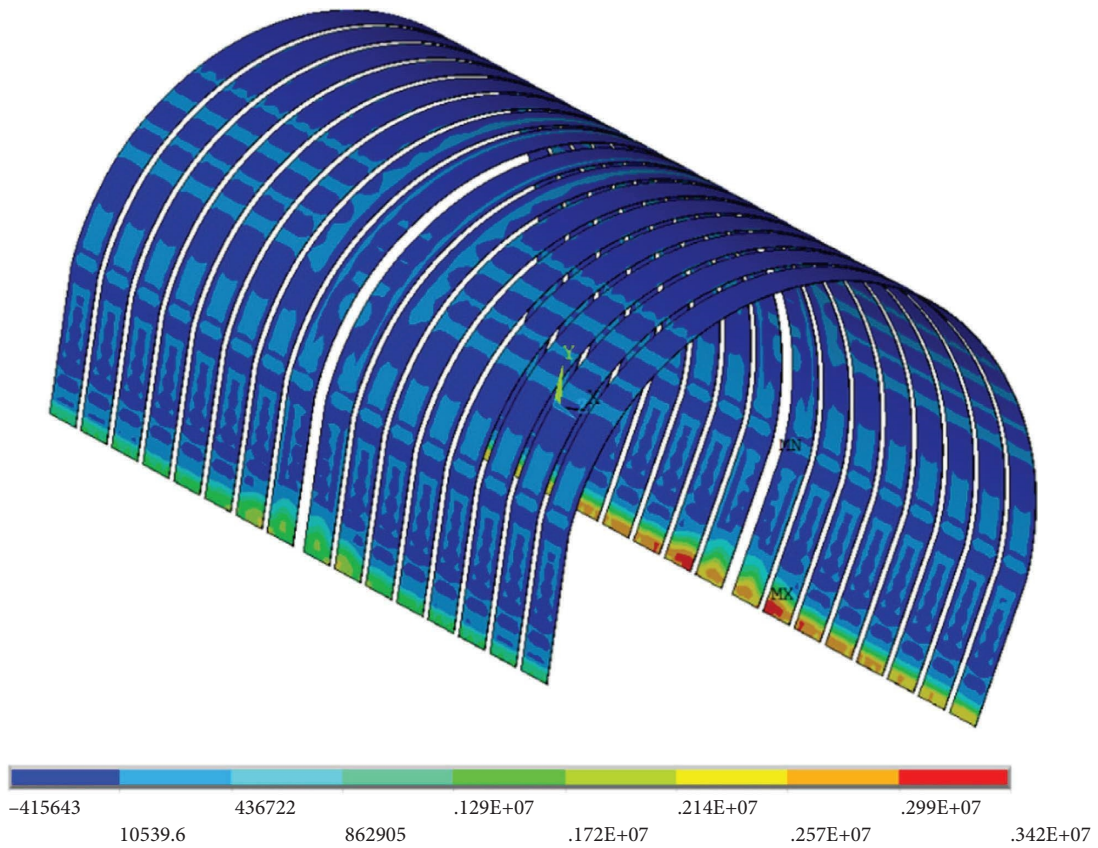


FIGURE 17: Stress diagram of steel plate with H125 steel frame.



FIGURE 18: Installation site of steel arch.



FIGURE 19: Installation site of connecting reinforcement and steel plate.

5. Conclusions and Further Observations

5.1. Conclusions

- (1) The lining disease of narrow double-track heavy-haul railway tunnel can be repaired with limited maintenance “window” time without affecting the normal operation of the catenary and power supply facilities. This technology has great practical significance and broad application prospect.

- (2) When H175 and H125 steel frames with an arrangement spacing of 1 m were used, the steel frame, steel plate, and concrete met the material tensile strength requirements set out in the *Code for Design of Railway Tunnel of China* (TB 10003-2016), indicating that the lining steel arch frame reinforcement structure of “circumferential H-section steel + welded steel plate between arches + filled concrete between slab walls” for a double-track railway tunnel is feasible as a whole.

5.2. Further Observations. Through theoretical analysis and numerical simulation, the compressive strength of the reinforced structure of a lined steel arch frame in a double-track railway tunnel was analyzed, and the applicability and effectiveness of the reinforcement scheme were verified by field work. Although some conclusions were drawn, this paper had limitations due to time and conditions.

- (1) This paper only analyzed the tensile capacity of each component of the reinforced structure and did not compare and analyze the stress state of the lining before and after reinforcement. In the next step, changes to the stress state of lining before and after reinforcement will be studied in depth.
- (2) In the field verification, long-term health monitoring of the reinforced structure was not carried out. In subsequent research, sensors will be installed in the reinforced structure for real-time health monitoring.

6. Conclusion

- (1) The technology is simple and can effectively repair the defects of railway tunnel bottom structure under the conditions of narrow site, short time of maintenance skylight, strict requirements of track size variation, and no interference with normal operation of train, which has great significance and broad application prospect.
- (2) The drainage system of the existing railway tunnel bottom can be applied to the bottom structure renovation of railway tunnel. The high-strength transverse diversion structure at the bottom of the tunnel has the advantages of strong bearing capacity, high drainage capacity, and corrosion resistance, which can provide reference for the subsequent implementation of the reconstruction project of the bottom structure of railway tunnel.

Data Availability

The data used to support the findings of this study are included within the article.

Conflicts of Interest

The authors declare that there are no conflicts of interest regarding the publication of this paper.

Authors' Contributions

Weibin Ma and Jinfei Chai contributed to the central idea, analyzed most of the data, and wrote the initial draft of the paper. Xiaoyan Du interpreted the result. Yao Li contributed to the project overview and cause analysis. Peng Zhao contributed to the analyses. All authors discussed the results and revised the manuscript.

Acknowledgments

The authors would like to thank Dr. Hao Sun from Beijing University of Science and Technology for his support in the numerical simulation in this paper. This study was supported by the Science and Technology Innovation Project of National Energy Investment Group Co., Ltd., grant no. GJNY-20-231. The authors are grateful for the support.

References

- [1] J. F. Gong, G. R. Tang, and W. Wang, "Statistics of China's railway tunnels by the end of 2021 and design & construction overview of gaoligongshan tunnel," *Tunnel construction (Chinese and English)*, vol. 42, no. 3, pp. 508–517, 2022.
- [2] C. F. Lu, "Maintenance mode and key technology of high speed railway bridge and tunnel engineering," *China Railway*, vol. 7, pp. 1–8, 2017.
- [3] W. B. Ma, J. F. Chai, D. G. Cai et al., "Research on in situ stress distribution of the railway tunnels in southwest China based on the complete temperature compensation technology," *Shock and Vibration*, vol. 2021, Article ID 7170850, 14 pages, 2021.
- [4] W. B. Ma, J. F. Chai, Z. F. Zhu et al., "Research on vibration Law of railway tunnel substructure under different axle loads and health conditions," *Shock and Vibration*, vol. 2021, Article ID 9954098, 14 pages, 2021.
- [5] W. B. Ma, J. F. Chai, Z. L. Han et al., "Research on design parameters and fatigue life of tunnel bottom structure of single-track ballasted heavy-haul railway tunnel with 40-ton axle load," *Mathematical Problems in Engineering*, vol. 2020, Article ID 3181480, 9 pages, 2020.
- [6] Z. L. Han, W. B. Ma, J. F. Chai et al., "A treatment technology for optimizing the stress state of railway tunnel bottom structure," *Shock and Vibration*, vol. 2021, Article ID 9191232, 13 pages, 2021.
- [7] J. F. Chai, "Research on dynamic response characteristics for basement structure of heavy haul railway tunnel with defects," *Mathematics*, vol. 9, no. 22, p. 2893, 2021.
- [8] J. F. Chai, "Research on multijoint rock failure mechanism based on moment tensor theory," *Mathematical Problems in Engineering*, vol. 2020, Article ID 6816934, 17 pages, 2020.
- [9] G. Q. Zhao, "Treatment method of cracking in railway tunnel lining," *Chinese Journal of Rock Mechanics and Engineering*, vol. 15, no. 4, pp. 385–389, 1996.
- [10] J. Cheng, J. S. Yang, and N. Cao, "Study on crack remediation and reinforcement to lining in railway tunnel," *Journal of Safety Science and Technology*, vol. 10, no. 9, pp. 134–139, 2014.
- [11] D. Z. Cheng, *Study on the Lining Crack Disease of Tunnel and its Control Measures in High Speed Railway*, Ph.D. Thesis, Central South University, Changsha, China, 2012.
- [12] Y. B. Niu, Q. L. Zhang, and W. B. Ma, "The Generating mechanism and control measures for disease of heavy-haul railway tunnel," *Railway Engineering*, vol. 56, no. 7, pp. 34–37, 2012.
- [13] D. Y. Yu, *Study of Safety Evaluation and Treatment Measures of Cavity Defects behind Railway Tunnel Lining*, China Academy of railway sciences, Beijing, China, 2019.
- [14] H. J. Ma, S. M. Tian, and B. X. Fu, "Application and development of corrugated pipe(plate) technology for railway engineering," *China Railway*, vol. 1, pp. 91–101, 2019.
- [15] Q. Wu, P. P. Peng, and Y. M. Cheng, "The interpolating element-free Galerkin method for elastic large deformation problems," *Science China Technological Sciences*, vol. 64, no. 2, pp. 364–374, 2021.
- [16] H. Cheng, M. J. Peng, Y. M. Cheng, and Z. Meng, "The hybrid complex variable element-free Galerkin method for 3D elasticity problems," *Engineering Structures*, vol. 219, Article ID 110835, 2020.
- [17] J. Li and J. Wu, "Study on elastoplastic damage constitutive model of concrete I: basic formula," *Journal of Civil Engineering*, vol. 38, pp. 14–20, 2005.